4. REMARKS ON OBLATE SPHEROID

The calculations of Sec. 2 apply to oblate as well as to prolate spheroids. In this case too one has therefore just the curling, represented by (7), the coherent rotation which is known, and the mode analogous to the buckling treated in Sec. 3, which can be readily represented by transforming (11), (14), and (15) to oblate spheroidal coordinates. The fact that the curves in Fig. 1 cut at the sphere shows that for oblate spheroids the mode shown in Fig. 1 is higher than the curling, since it seems unlikely that the curves would cross again. However, it is possible that one of the other eigenvalues, which is larger for prolate spheroids, would also cross these curves at the sphere, and would thus become smaller than curling for oblate spheroids, so that there still exists the possibility of a third mode. For lack of adequate tabulation of the oblate functions, this possibility could not be checked.

ACKNOWLEDGMENT

Most of the numerical computations have been carried out by C. Abraham.

PHYSICAL REVIEW VOLUME 131, NUMBER 4 15 AUGUST 1963

Size Effects in the Resistivity of Indium Wires at 4.2°K

R. T. BATE, BYRON MARTIN,* AND P. F. HILLE
Battelle Memorial Institute, Columbus, Ohio
(Received 18 March 1963)

Measurements are reported of the dependence of the resistance (at 4.2°K) of high-purity polycrystalline indium wires on the wire diameter. Data, which were taken on recrystallized wires extruded through dies of various sizes, and also on a single extruded wire gradually reduced in diameter by etching, are compared with those of Olsen. It is pointed out that any variation of the bulk electron free path over the Fermi surface must be taken into account in the analysis of size effect data on wires unless they are extremely small in diameter. A calculation of the size effect at 0°K in monocrystalline wires and in "unidimensionally" polycrystalline wires having a diameter large compared to the mean free path is made for an arbitrary Fermi surface and free path anisotropy. The result of the calculation for the polycrystalline case, which is limited to metals having isotropic bulk conductivities, is similar to the Fuchs-Dingle result for the isotropic case except that the effective resistivity is much more strongly size dependent when a large mean free path anisotropy exists. It is concluded on the basis of this derivation that the size effect data on indium wires and anomalous skin effect data can be reconciled if a large anisotropy in the mean free path exists.

INTRODUCTION

THE dependence of the resistance of circular wires on diameter has been studied theoretically[1–7] and also experimentally[6,8,9] for several metals. Experimental data of this type have frequently been analyzed by means of the Nordheim-Fuchs-Dingle[1,2] formula,

$$\rho_{\text{eff}}=\rho_b+\alpha\rho_b l/d\,, \qquad (1)$$

which (assuming diffuse surface scattering) expresses the effective resistivity, ρ_{eff}, of the wire in terms of the bulk resistivity, ρ_b, the mean free path, l, and the diameter, d. α is a dimensionless function of l/d which is unity in the Nordheim formula and varies from 0.75 to 1 as l/d goes from zero to infinity in the Fuchs-Dingle formulation. Equation (1) is often used to calculate the product $\rho_b l$ and the mean free path from size effect data.[10] The value of $\rho_b l$ obtained in this way is usually considerably larger than the value derived from anomalous skin effect data on polycrystalline samples.

The purpose of this paper is to report measurements of the size effect in polycrystalline indium wires and to point out that Eq. (1) is not applicable to these data. An equation similar to (1) [Eq. (1c)], which is believed to be valid for the residual resistivity of thick "one-dimensionally" polycrystalline wires of metals having arbitrary Fermi surfaces and an arbitrary dependence of the free path $l(k_f)$ (averaged over all final wave vectors), on the initial wave vector is derived. This formula is probably more appropriate to the case of "annealed" polycrystalline wires than is Eq. (1).

* Present address: Department of Physics, Ohio State University, Columbus, Ohio.

[1] K. Fuchs, Proc. Cambridge Phil. Soc. **34**, 100 (1938).
[2] R. B. Dingle, Proc. Roy. Soc. (London) **A201**, 545 (1950).
[3] E. H. Sondheimer, Suppl. Phil. Mag. **1**, 1 (1952).
[4] B. Luthi and P. Wyder, Helv. Phys. Acta **33**, 667 (1960).
[5] F. J. Blatt and H. G. Satz, Helv. Phys. Acta. **33**, 1007 (1960).
[6] B. N. Alexandrov and M. I. Kaganov, Zh. Eksperim. i Teor. Fiz. **41**, 1333 (1961)[translation: Soviet Phys.—JETP **14**, 948 (1962)]. The result appearing here differs from ours by a factor of $\hbar^2$ because we consider the Fermi surface in κ space rather than the similar surface in ρ space.
[7] M. Ya. Azbel' and R. N. Gurzhi, Zh. Eksperim. i Teor. Fiz. **42**, 632 (1962) [translation: Soviet Phys.—JETP **15**, 1133 (1962)].
[8] J. L. Olsen, Helv. Phys. Acta **31**, 713 (1958).
[9] L. R. Weisberg and R. M. Josephs, Phys. Rev. **124**, 36 (1961).
[10] J. L. Olsen, *Electron Transport in Metals* (Interscience Publishers, Inc., New York, 1962), Chap. 4, p. 84.

SAMPLE PREPARATION

The indium wires were prepared by extruding samples of indium through dies of various diameters. Information on the origin of the samples is given in the first column of Table I. Four die sizes were used (5, 10, 20, and 40 mil). Immediately after extrusion, the wires consisted of large numbers of fine crystallites, as shown in Fig. 1. However, it was found that a gradual recrystallization occurred if the wires were allowed to stand at room temperature, and this process was accompanied by a gradual decrease in the resistance measured at 4.2°K. This downward drift of resistance stopped after about a month and the final 4.2°K resistance was about 90% of the initial value. (All of the values reported are "final" values.) Annealing at higher temperatures did not markedly accelerate this recrystallization process. After this recrystallization period, the wires consisted of much larger crystallites as shown in Fig. 2. Since the wires employed ranged between 6 in. and several feet in length, all of the wires still contained at least several hundred crystallites after recrystallization.

TABLE I. Samples and results.

Sample designation	Source	Diameter (mm)	$10^4 r_{4.2}/r_{273}$[a]	l_0[b] (mm)	Symbol
Tadanac (T)	Cominco Products, Inc.	∞[c]	(0.66)	(0.113)	□
		0.508	1.053		
		0.254	1.432		
		0.127	2.283		
C	Unknown	∞	(1.02)	(0.072)	○
		0.508	1.374		
		0.254	1.806		
		0.127	2.600		
Incoa A	Indium Corp. of America	∞	2.78	0.0266	△
		0.508	3.11		
		0.254	3.40		
		0.127	4.06		
Incoa B	Indium Corp. of America	∞	2.71	0.0273	▽
		0.508	3.01		
		0.254	3.31		
		0.127	4.03		
Incoa C	Indium Corp. of America	∞	2.98	0.0250	▲
		0.508	3.34		
		0.254	3.61		
		0.127	4.33		
Incoa E (Etched)	Indium Corp. of America	∞	2.86	0.0260	+
		0.510	3.17		
		0.452	3.28		
		0.426	3.22		
		0.392	3.31		
		0.359	3.32		
		0.298	3.42		
		0.264	3.51		
		0.200	3.78		
		0.156	3.92		

[a] Ratio of resistance at 4.2°K to that at 273°K times 10^4.
[b] Bulk mean free path.
[c] Values listed for infinite diameters are bulk values obtained by an extrapolation described in the text. Values in parentheses are somewhat uncertain.

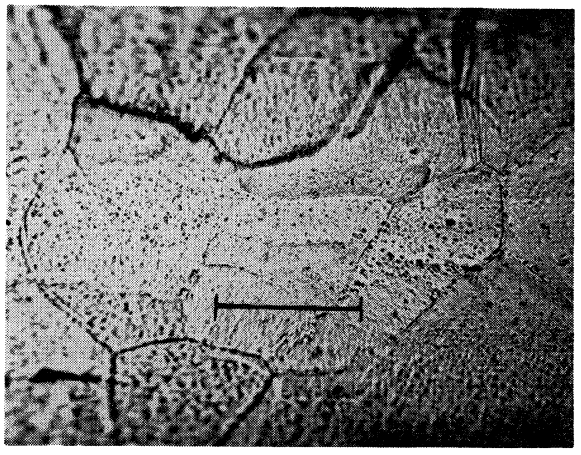

FIG. 1. Photomicrograph of a portion of indium wire etched immediately after extrusion. Note the relatively small size of the crystallites. Scale indicates 0.1 mm.

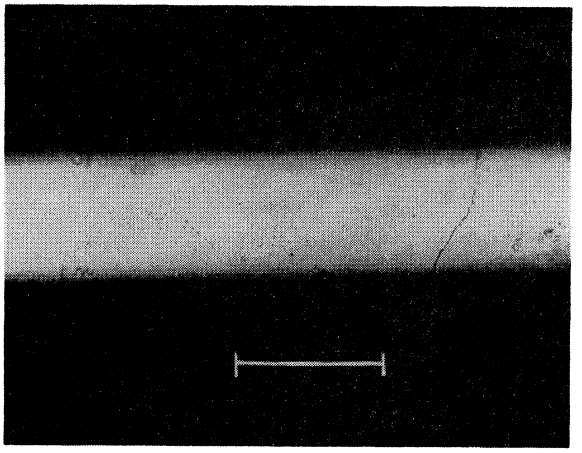

FIG. 2. Photomicrograph of indium wire etched approximately a month after extrusion. The crystallites are now so large that the wire can be considered a "chain" of single crystals. Scale indicates 0.1 mm.

It is important to note that although the recrystallized wires consist of numerous crystallites which are presumably randomly oriented, they are not truly polycrystalline in a three-dimensional sense. A line passed through the wire perpendicular to its axes will probably not intersect a grain boundary. Only lines nearly parallel to the axis will intersect a large number of grain boundaries in the wire. This configuration, which might appropriately be called "coarse" or "one-dimensional" polycrystallinity, is probably similar to that attained in thin annealed wires of many metals. This distinction between "one-dimensional" and "three-dimensional" polycrystallinity must be considered in the analysis of experimental results.

Although the results on extruded wires seemed self-consistent, the possibility existed that a radially inhomogeneous distribution of impurities introduced during extrusion could give rise to systematic errors in the measurements. To check on this possibility, a 20-mil wire was gradually reduced in diameter by etching in dilute aqua regia. Resistivity measurements were made after each etching step. The size dependence obtained in this manner agreed perfectly with that obtained on extruded wires of different diameters.

EXPERIMENTAL PROCEDURE

Resistivity measurements were made by a four-terminal technique employing a Leeds and Northrup

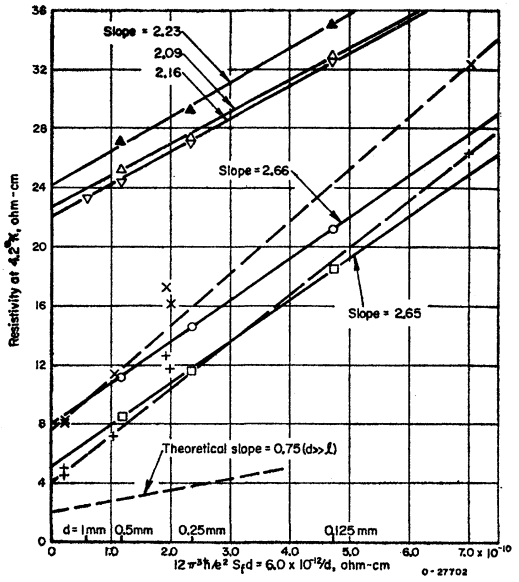

FIG. 3. Size dependence of the effective resistivity of indium wires at 4.2°K. The abscissa is $\rho_b l_0/d$, assuming $\rho_b l_0 = 0.6\times10^{-11}$ Ω-cm². The symbols for our samples are identified in Table I. The symbols for Olsen's data (dashed lines) are: ×, 4.2°K, +, extrapolated to 0°K.

K-3 potentiometer for potential measurements. The wires were enclosed in a Pyrex tube, filled with helium gas. This tube was inserted into an ice bath or directly into the helium storage Dewar depending on the temperature at which the measurements were to be made. The current was reversed to eliminate thermoelectric voltages, and data were taken at several currents to eliminate the possibility of sample heating. The wire diameters were measured with a microscope provided with a calibrated eyepiece and were checked against the ice temperature resistance.

RESULTS

The results are tabulated in Table I. Estimates of the bulk resistance ratios have been made by extrapolating to infinite diameter. (See Fig. 3.) Because of the uncertainty involved in this procedure, the bulk values for the two purest samples, T and C, are probably not very accurate.

DISCUSSION

According to Eq. (1) a plot of ρ_{eff} versus $\rho_b l/d$ should give a straight line, with a slope of unity in Nordheim's approximation. In the Fuchs-Dingle approximation, the same result should be found for $l \gg d$, but for $l \ll d$, the slope will be 0.75, with a gradual transition between the two cases when $l \sim d$. The quantity $\rho_b l$, which is a constant of the metal, can be obtained from anomalous skin effect data on polycrystalline samples by means of the relation,

$$\rho_b l = \frac{10^{18}}{4\sqrt{3}\pi^3\nu^2\Sigma^3} \simeq \frac{10^{18}}{215\nu^2\Sigma^3}, \qquad (2)$$

where ρ_b is measured in Ω cm, l in cm, and Σ is the surface conductivity in Ω^{-1} at a frequency ν in the "extreme anomalous range". It is also possible in principle to obtain values of $\rho_b l$ from measurements on thin wires and films. A summary of some published results for indium obtained by these various techniques is given in Table II.

TABLE II. Values of $\rho_b l_0$ for indium obtained by various methods.

Method	$\rho_b l_0$ (Ω-cm²)	Investigator
Anomalous skin effect	0.89×10^{-11}	Roberts[a]
Anomalous skin effect	0.6×10^{-11}	Dheer[b]
Cylindrical wires	1.4×10^{-11}	Olsen[c]
Thin film	2.0×10^{-11}	Toxen[d]
Theoretical[e]	0.54×10^{-11}	

[a] T. E. Faber, Proc. Roy. Soc. (London) **A241**, 531 (1952).
[b] E. A. Davies, Proc. Roy. Soc. (London) **A155**, 407 (1960).
[c] J. L. Olsen, *Electron Transport in Metals* (Interscience Publishers, Inc., New York, 1962), Chap. 4, p. 84.
[d] A. M. Toxen, Phys. Rev. **123**, 442 (1961).
[e] Calculated assuming three conduction electrons per atom and a spherical Fermi surface.

Examination of this table reveals that the values of $\rho_b l$ obtained from size effect data are considerably larger than those derived from the anomalous skin resistance. The anomalous skin effect values are in reasonable agreement with the free-electron model assuming 3 electrons/atom.

Since the magnetoacoustic data of Chandrasekhar and Rayne[11] suggest a Fermi surface for indium very similar to that predicted by the free-electron model, it would appear that the values of $\rho_b l$ obtained from size effect data are somewhat suspect. There is some indication in the literature that 0.6×10^{-11} Ω-cm² may be the most accurate anomalous skin effect value, and it agrees fairly well with the free-electron model,[12] so we have arbitrarily chosen this as the "true" value of $\rho_b l$.

Figure 3 shows a plot of[13] ρ_{eff} versus $0.6\times10^{-11}/d$ for wires extruded from the various samples. The data on the etched wire have been omitted for clarity. The data of Olsen[8] at 4.2°K and also his extrapolations to 0°K are plotted for comparison.

The points for each sample lie on straight lines on this type of plot, those for the more pure samples having a slightly larger slope. The slope for Olsen's sample, which had a bulk resistivity about the same as our sample C, is larger than that for sample C both at 4.2 and 0°K. The reason for the difference in slope at 4.2°K, between our sample and Olsen's is not known but the

[11] J. A. Rayne and B. S. Chandrasekhar, Phys. Rev. **125**, 1952 (1962).
[12] In aluminum, which has a Fermi surface very similar to that of indium, the anomalous skin effect result agrees perfectly with the prediction of the free-electron model. [E. Fawcett, in *The Fermi Surface*, edited by W. A. Harrison and M. B. Webb (John Wiley & Sons, Inc., New York, 1960), p. 197.]
[13] Determined from the resistance ratios using $\rho_{273} = 8.1\times10^{-6}$ Ω-cm.

increase in slope between 0 and 4.2°K has been attributed to an enhanced effect of electron-phonon scattering on the resistivity due to boundary scattering.[4,5,7,8] (The larger slope for our samples C and T may also be a result of this phenomenon.)

Using the bulk resistivity values (listed in Table I) obtained by extrapolation of the lines in Fig. 3 to infinite diameter (i.e., to zero on the abscissa), and employing the result, $\rho_b l = 0.6\times10^{-11}$ Ω-cm^{-2} we have calculated the bulk mean free paths for each sample. These values are also listed in Table I. Knowledge of the mean free path permits the construction of a universal plot based on the relation [obtained by dividing Eq. (1) by ρ_b]:

$$\rho_e/\rho_b = 1+\alpha l/d. \tag{1a}$$

Plotting ρ_e/ρ_b versus l/d should yield a universal curve which approaches a straight line with slope $\frac{3}{4}$ as l/d approaches zero.

A plot of this type for the less pure samples is shown in Fig. 4. The data on samples "C" and "T" are omitted because of the uncertainty in the determination of ρ_b by extrapolation, but the data on the wire reduced in diameter by etching have been included. When plotted in this way, the data lie on a straight line with a slope of $(2.9)\times\frac{3}{4}\simeq 2.2$. The slope of the Fuch's-Dingle relation (1a) increases from 0.75 ($l/d=0$) to about 0.88 over the range of l/d covered by the data. Thus the slope of the experimental line is between two and three times that predicted by the Fuch's-Dingle relation if $\rho_b l = 0.6\times10^{-11}$ Ω-cm^2, and an equation of the form,

$$\rho_{\text{eff}}/\rho_b = 1+\gamma\alpha l/d \tag{1b}$$

is suggested, where γ lies between 2 and 3.

The Fuchs-Dingle formula was derived assuming a spherical Fermi surface and an isotropic relaxation time, and it is usually implied that the result is valid for the residual resistance of a polycrystalline wire even though the initial assumptions are incorrect for the metal in question. If we pass over the question of grain boundary scattering, it seems that the result should be valid if the electron traverses several crystallites between encounters with the surface of the wire. However, in the case of "one-dimensional" polycrystallinity, where the average distance between grain boundaries is large compared to the bulk mean free path, most of the electrons do not traverse more than one or two crystallites between encounters with the surface, and the Fuchs-Dingle result does not apply.

The correct result for this case is obtained by calculating the size effect for a monocrystalline wire allowing the Fermi surface and mean free path anisotropy to be arbitrary and then using the fact that the resistance of the polycrystalline wire is essentially the sum of the resistances of the individual crystallites when the length of the crystallites is large compared to the bulk free path. The calculation is carried out in Appendixes I and II and the result for a cubic metal or one in which the conductivity is isotropic[14] is

$$\rho_{\text{eff}}/\rho_b = 1+\langle l^2\rangle/\langle l\rangle^2\tfrac{3}{4}\bar{l}/d, \quad (\bar{l}\ll d, \bar{d}_g), \tag{1c}$$

where

$$\langle l\rangle\equiv\bar{l}=\int l(k_f)dS_f/S_f, \quad \langle l^2\rangle=\int l^2(k_f)dS_f/S_f,$$

the integrals being taken over the Fermi surface. (The symbol $\bar{d}_g$ signifies the average distance between grain boundaries.) Comparing (1b) with (1a) and noting that $\alpha=\frac{3}{4}$ for $l\ll d$, we see that for thick wires, γ in (1b) is given by

$$\gamma=\langle l^2\rangle/\langle l\rangle^2,$$

which is unity if the mean free path is constant but is always greater than unity if the mean free path is a function of $\mathbf{k}_f$, the wave vector at the Fermi surface.

Thus the apparent discrepancy between the size effect data on wires and the anomalous skin effect data can be understood if a large mean free path anisotropy exists. (The meaning of the word "anisotropy" as it is used here has been generalized.[15]) However, since our measurements were made at 4.2°K, the resistivity values we obtained are not the residual resistivities. Because of the effect suggested by Olsen[8] and discussed by several others,[4,5,7] the slopes of our curves in Figs. 3 and 4 are larger than they would have been if the measurements had been made at very low temperatures. This means that a correction, the magnitude of which can be estimated roughly by comparison of Olsen's 4.2 and 0°K (extrapolated) curves in Fig. 4, should be applied to our data in order to find the slope corresponding to the residual resistivity.

Although we have no reliable way of calculating this correction, we can see that it must be fairly small for the wires represented in Fig. 4, because they had bulk resistivities more than twice as large as Olsen's sample.

---

[14] Although indium is not quite cubic, the conductivity anisotropy at 273°K is only about 5%.

[15] The crystallite orientation in the wires is probably not completely random, but the influence of a preferred crystallite orientation on the result may not be as great as one would at first suppose, at least for cubic multivalent metals. This is because the controlling factor in the size effect is the variation of the mean free path *over the Fermi surface*. If the Fermi surface is re-entrant or consists of more than one sheet, as it does in multivalent metals, then electrons at several points on the Fermi surface characterized by different mean free paths may be moving in the same direction. Thus, anisotropy over the Fermi surface does not necessarily imply spatial anisotropy, but only the spatial anisotropy of the mean free path leads to a dependence of the size effect on orientation. A hypothetical case which would exhibit a variation of mean free path over the Fermi surface without spatial anisotropy would be a semimetal possessing two spherical bands characterized by different mean free paths. This case can be handled exactly by an extension of the Fuchs-Dingle formula and the result for *thick* wires is idential with Eq. (B7). However, for very thin wires, Eq. (1) (with $\alpha=1$) holds. Since these results are valid for single crystals and for unidimensionally polycrystalline wires regardless of any preferred orientation, we see that spatially anisotropic mean free path is not a necessary condition for the validity of (B7) with $\langle l^2\rangle/\langle l\rangle^2>1$ and that, when the spatial anisotropy is slight, the existence of a preferred orientation of crystallites will have little effect on the results.

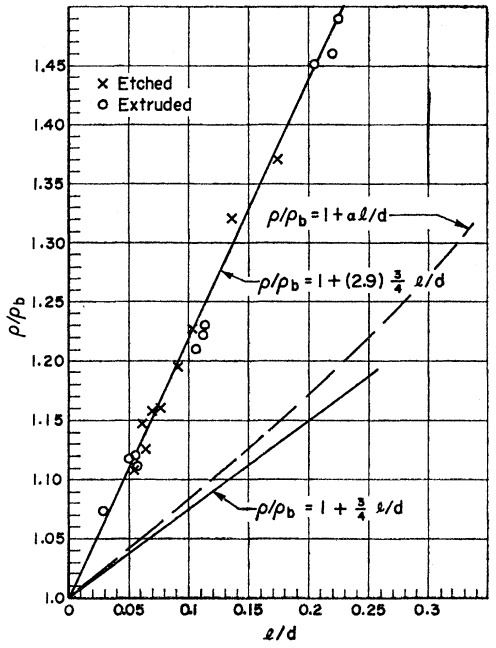

FIG. 4. Comparison of size dependence of the effective resistivity of indium wires at 4.2°K with that predicted by the Fuchs-Dingle relation.

Allowing roughly for this correction, one must still have $\gamma\sim 2$ to bring the size effect data and the anomalous skin effect data into agreement. Some supporting evidence for anisotropic mean free paths in indium is found in the high-field magnetoacoustic attenuation data of Chandrasekhar and Rayne.[11]

ACKNOWLEDGMENTS

The authors are grateful to Dr. E. M. Baroody for his assistance and comments, particularly in connection with the Appendices, and to Professor R. G. Chambers, for a discussion of some details of the derivations. We are also indebted to Battelle Memorial Institute for financial support.

APPENDIX A

Approximate Calculation of the Residual Resistance of Monocrystalline Wires for an Arbitrary Fermi Surface and Mean Free Path Anisotropy and Assuming Diffuse Surface Scattering

The bulk conductivity, along the ith principal axis of the conductivity tensor of an impure metal at 0°K, is given approximately by

$$\sigma_b{}^i=\frac{e^2}{4\pi^3\hbar}\int(\mathbf{s}\cdot\mathbf{b}_i)^2 l_0(\mathbf{k}_f)dS_f, \tag{A1}$$

where $\mathbf{s}$ is a unit vector parallel to the direction of motion of an electron [i.e., parallel to $\mathbf{v}_f(=\hbar^{-1}\,\mathrm{grad}_k\epsilon$, at $\mathbf{k}_f$ on the Fermi surface)], $\mathbf{b}_i$ is a unit vector parallel to the ith principal axis, and $l_0(\mathbf{k}_f)$ is the mean distance traveled between scattering events by an electron having a wave vector $\mathbf{k}_f$. (The subscript 0 is omitted in the body of the article.) The integration is over the Fermi surface in wave vector space. For a cubic metal, or one in which the conductivity is isotropic, (A1) reduces to

$$\sigma_b=\frac{e^2}{12\pi^3\hbar}\int l_0(\mathbf{k}_f)dS_f=\frac{e^2}{12\pi^3\hbar}\bar{l}_0 S_f, \tag{A2}$$

where

$$\bar{l}_0=\int l_0(\mathbf{k}_f)dS_f/S_f \tag{A3}$$

is the bulk mean free path and S_f is the area of the Fermi surface in wave vector space.

Chambers[16] has pointed out that the conductivity of a wire for the case of a spherical Fermi surface and isotropic mean free path can be calculated from a "kinetic theory" formula, and that the result is the same as that obtained from the solution of the Boltzmann equations in the relaxation time approximation by Fuchs and Dingle,[12] if the free path at a point in the wire is taken to be

$$l=l_0(1-e^{-OP/l_0}), \tag{A4}$$

where OP is the distance from the point to the surface of the wire measured along the direction of motion of the electron, and the surface scattering is assumed to be diffuse.

An obvious generalization of Chambers' argument to the case of an arbitrary Fermi surface and an arbitrary mean free path anisotropy is to calculate the contribution of a volume element at a point O in the wire to the total conductance by means of formula (A1) with $l_0(\mathbf{k}_f)$ replaced by

$$l_{\mathrm{eff}}(\mathbf{k}_f)=l_0(\mathbf{k}_f)(1-e^{-OP/l_0(\mathbf{k}_f)}). \tag{A5}$$

Let dA be an increment of area on the cross section (perpendicular to the wire axis) of the wire shown in Fig. 5, and consider the volume element generated by projecting dA parallel to the wire axis. The contribution of this volume element to the *conductance* (per unit length) of the wire is

$$d\Sigma_i=\frac{e^2}{4\pi^3\hbar}\int(\mathbf{s}\cdot\mathbf{b}_i)^2 l_0(\mathbf{k}_f)(1-e^{-OP/l_0})dS_f dA, \tag{A6}$$

where $\mathbf{b}_i$ is parallel to the wire axis (i.e., if the conductivity is not isotropic, then we require that the wire axis be parallel to a principal axis of the conductivity tensor). If θ is the angle between $\mathbf{s}$ and $\mathbf{b}_i$ (see Fig. 5) then the effective conductivity of the wire is given by

$$\sigma_e{}^i=\frac{1}{\pi a^2}\left(\frac{e^2}{4\pi^3\hbar}\right)\int\int\cos^2\theta\, l_0(k_f)\times(1-e^{-OP'/l_0\sin\theta})dS_f dA, \tag{A7}$$

[16] R. G. Chambers, Proc. Roy. Soc. (London) **A202**, 378 (1950).

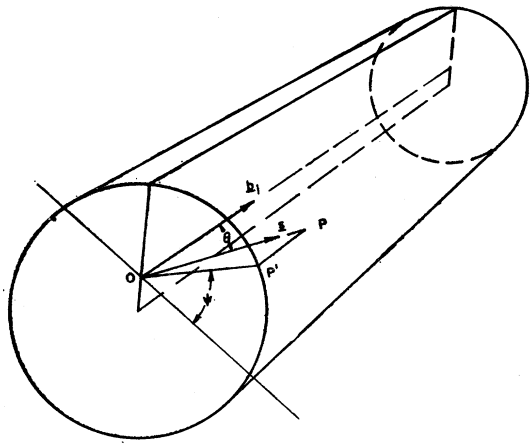

FIG. 5. Geometrical construction used in calculating resistivity of monocrystalline wire. The electron under consideration is located at O and is moving in the direction OP. $\mathbf{b}_i$ is parallel to the axis of the wire and to a principal axis of the bulk conductivity tensor.

where a is the radius of the wire and OP' is the projection of OP on the cross section through O. For O fixed, OP' is a function of the azimuthal angle, Ψ (see Fig. 5). If we now interchange the order of integration in (A7), we can keep the angles θ and Ψ which specify the direction of OP fixed while O sweeps over the cross section. Thus, we obtain

$$\sigma_{e^i}=\left(\frac{e^2}{4\pi^3\hbar}\right)\int \cos^2\theta l_0(k_f) \times\left[\frac{1}{\pi a^2}\int(1-e^{-OP'/l_0\sin\theta})dA\right]dS_f. \quad \text{(A8)}$$

The expression in brackets in (A8), which we call $I(\beta)$, can be shown to reduce to

$$I(\beta)=1-\frac{4}{\pi\beta}[1-J(\beta)], \quad \text{(A9)}$$

where

$$J(\beta)=\int_0^{\pi/2} e^{-\beta\sin\gamma}\sin\gamma d\gamma \quad \text{(A10)}$$

and $\beta=d/[l_0(k_f)\sin\theta]$, $d=2a$. The properties of $J(\beta)$ can be summarized as follows[17]:

$$J(\beta)\to\beta^{-2}, \quad \beta>10 \quad \text{(A11)}$$

$$J(\beta)\to 1-\tfrac{1}{4}\pi\beta+\tfrac{1}{3}\beta^2, \quad \beta\ll 1. \quad \text{(A12)}$$

Also,

$$J(\beta)\simeq\left[I_0(\beta)+\frac{2}{3}I_2(\beta)-\frac{2}{15}I_4(\beta)+\frac{2}{35}I_6(\beta)-\frac{2}{63}I_8(\beta)+\cdots\right]-\frac{\pi}{2}I_1(\beta) \quad \text{(A13)}$$
$$=\tfrac{1}{2}\pi[L_1(\beta)-I_1(\beta)]+1,$$

where I_n are modified Bessel functions of the first kind, and $L_1(\beta)$ is a modified Struve function. A discussion of $J(\beta)$, and of some closely related functions, as well as a rather complete tabulation of $J(\beta)$ has been given by Müller.[18] Some values of $I(\beta)$ which are accurate to three significant figures are given in Table III.

TABLE III. Selected values of the function $I(\beta)=1-(4/\pi\beta)\left(1-\int_0^{\pi/2} e^{-\beta\sin\gamma}\sin\gamma d\gamma\right)$.

β	$I(\beta)$
0	0
0.5	0.184
1.0	0.323
1.5	0.430
2.0	0.512
3.0	0.629
4.0	0.705
5.0	0.756
10.0	0.874

If $d/l_0\ll 1$ (thin wire), then $\beta(=d/l_0\sin\theta)$ is also $\ll 1$ except when θ is small. For *very* thin wires, the contribution from portions of the Fermi surface where β is not small should be negligible and substituting (A12) and (A9) into (A8) should be a good approximation. The result of this substitution is

$$\sigma_{e^i}\to\left(\frac{e^2}{4\pi^3\hbar}\right)\left(\frac{4d}{3\pi}\right)\int\frac{\cos^2\theta}{\sin\theta}dS_f, \quad \left(\frac{d}{l_0}\to 0\right) \quad \text{(A14)}$$

a result given (without derivation) by Alexandrov and Kaganov.[6]

As to the accuracy of Eq. (A14), one can ask whether it is correct in the limit as $d/l_0\to 0$, and, if so, for what range of d/l_0 does it provide a sufficiently good approximation. The first part of the question can be answered with little detailed knowledge of the Fermi surface. For example, a finite value of the curvature of the surface at $\theta=0$ would be a sufficient condition for the correctness of the limit. The second part cannot be answered without more knowledge of the Fermi surface. For some small, but finite, value of d/l_0 one would need to estimate the error caused by the poor representation of $I(\beta)$ in the small θ region. This estimate cannot be made without some specific information on the value of the curvature near $\theta=0$. If one attempts to estimate corrections to (A14) by using further terms in the expansion (A12) [which can be obtained by expansion of the exponential in (A10)], it is found that the series obtained in place of (A14) diverges. This happens because the succeeding terms contain integrals similar to (A14) having higher powers of $\sin\theta$ in the denominator of the integrand. These integrals are in general unbounded. However, evaluation of approximate correc-

[17] We are indebted to E. M. Baroody and M. L. Glasser for these results.

[18] R. Müller, Z. Angew. Math. Mech. **19**, 36 (1939). (See p. 54.)

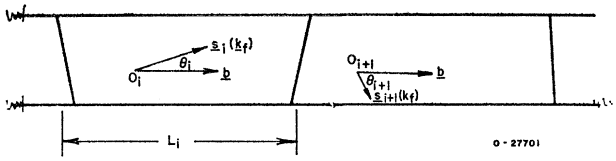

FIG. 6. Diagram of "unidimensionally" polycrystalline wire showing electron trajectories [along $\mathbf{s}_i(\mathbf{k}_f)$] corresponding to a given $\mathbf{k}_f$ in each crystallite. (The letter i is now the crystallite index.)

tions by other techniques indicates that (A14) will hold *only* for very small values of d/l_0.[19]

The conductivity of a thick wire ($d \gg l_0$) can be found by noting that, since $J(\beta)$ goes to zero as β^{-2} for large β,

$$I(\beta) \simeq 1-4/\pi\beta, \quad (d/l_0>10).$$

Substituting this into (A8) we obtain

$$\sigma_e{}^i \simeq \sigma_b{}^i - \left(\frac{e^2}{4\pi^3\hbar}\right)\left(\frac{4}{\pi d}\right)\int \cos^2\theta \sin\theta l_0^2 dS_f, \quad \left(\frac{d}{l_0}>10\right). \quad \text{(A15)}$$

APPENDIX B

Approximate Calculation of the Residual Resistance of a Thick "Unidimensionally" Polycrystalline Wire for Arbitrary Anisotropy but Cubic Symmetry

We assume that the average distance, $\bar{d}_g$, between grain boundaries is large compared to the mean free path and to the diameter of the wire. This situation is illustrated schematically in Fig. 6. The resistance of the wire in this case will be just the sum of the resistances of the individual monocrystalline sections which comprise it. The conductance of the ith crystallite is (from A8)

$$\frac{1}{R_i} = \frac{\pi d^2}{4L_i}\left(\frac{e^2}{4\pi^3\hbar}\right)\int \cos^2\theta_i l_0(\mathbf{k}_f) I(\beta_i) dS_f, \quad \beta_i = d/[l_0(\mathbf{k}_f)\sin\theta_i], \quad \text{(B1)}$$

where L_i is the length of the crystallite and θ_i is the angle between the velocity vector at $\mathbf{k}_f$ and the wire axis in the ith crystallite. The effective resistivity of a wire of length L is [using (A15)]

$$\rho_e = \frac{\pi d^2}{4L}\sum R_i = \left(\frac{4\pi^3\hbar}{e^2}\right) \times \sum_i \left[\frac{L_i/L}{\int \cos^2\theta_i l_0 dS_f - (4/\pi d)\int \cos^2\theta_i \sin\theta_i l_0^2 dS_f}\right] \quad \text{(B2)}$$

or [using (A1) and the cubic symmetry]

$$\rho_e \simeq \rho_b \sum_i (L_i/L)\left[1-\frac{12}{\pi d \bar{l}_0 S_f}\int \cos^2\theta_i \sin\theta_i l_0^2(k_f) dS_f\right]^{-1}, \quad \text{(B3)}$$

where

$$\bar{l}_0 = \int l_0(\mathbf{k}_f) dS_f/S_f.$$

When $l_0/d \ll 1$, the bracketed expression in (B3) is of the form,

$$[1-a]^{-1} \simeq 1+a, \quad (a \ll 1)$$

so that we can write

$$\rho_e \simeq \rho_b\left(1+\frac{12}{\pi \bar{l}_0 S_f d}\sum_i L_i/L \int \cos^2\theta_i \sin\theta_i l_0^2 dS_f\right). \quad \text{(B4)}$$

If we interchange the order of summation and integration in the second term of (B4) we must then consider the sum

$$\sum_i L_i/L \cos^2\theta_i \sin\theta_i. \quad \text{(B5)}$$

If the orientation of the crystallites is random,[15] this sum just becomes the average of $(\cos^2\theta \sin\theta)$ over a unit sphere (or over a solid angle of 4π):

$$\langle \cos^2\theta \sin\theta \rangle = \frac{1}{2}\int_0^\pi \cos^2\theta \sin^2\theta d\theta = \frac{\pi}{16}. \quad \text{(B6)}$$

Thus, (B4) becomes

$$\rho_e = \rho_b[1+\langle l_0^2\rangle/\langle l_0\rangle^2 \tfrac{3}{4}\bar{l}_0/d], \quad (\bar{l}_0 \ll d, \bar{d}_g) \quad \text{(B7)}$$

where

$$\langle l_0^2\rangle = \int l_0^2(k_f) dS_f/S_f.$$

[19] See also Chambers' discussion of the limiting case for thin films. [R. G. Chambers, Can. J. Phys. 34, 1395 (1956).]

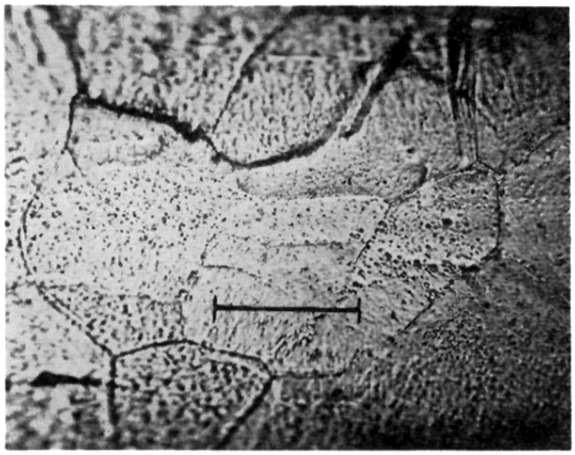

FIG. 1. Photomicrograph of a portion of indium wire etched immediately after extrusion. Note the relatively small size of the crystallites. Scale indicates 0.1 mm.

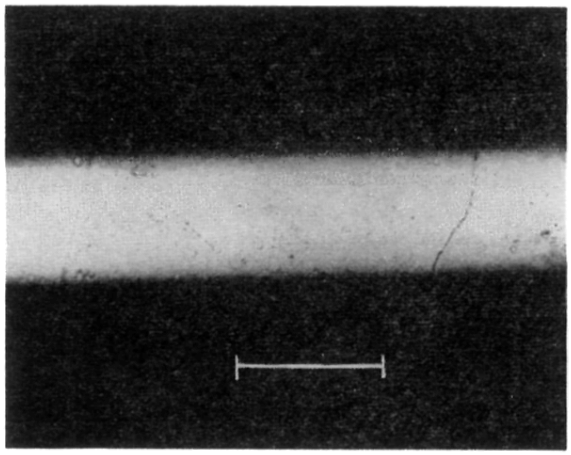

FIG. 2. Photomicrograph of indium wire etched approximately a month after extrusion. The crystallites are now so large that the wire can be considered a "chain" of single crystals. Scale indicates 0.1 mm.